Computer Methods and Programs in Biomedicine 254 (2024) 108305

Contents lists available at ScienceDirect

Computer Methods and Programs in Biomedicine

journal homepage: www.sciencedirect.com/journal/computer-methods-and-programs-in-biomedicine

EMG-based prediction of step direction for a better control of lower limb wearable devices

Eugenio Anselmino [a,*], Alberto Mazzoni [a], Silvestro Micera [a,b]

[a] Department of Excellence in Robotics and AI, Scuola Superiore Sant'Anna, The BioRobotics Institute, Pisa, Italy
[b] Bertarelli Foundation Chair in Translational Neuroengineering, EPFL, Genève, Switzerland

ARTICLE INFO

Keywords:
EMG
Intention decoding
Gait
Machine learning
Wearable devices

ABSTRACT

Background and objectives: Lower-limb wearable devices can significantly improve the quality of life of subjects suffering from debilitating conditions, such as amputations, neurodegenerative disorders, and stroke-related impairments. Current control approaches, limited to forward walking, fall short of replicating the complexity of human locomotion in complex environments, such as uneven terrains or crowded places. Here we propose a high-level controller based on two Support Vector Machines exploiting four surface electromyography (EMG) signals of the thigh muscles to detect the onset (Toe-off intention decoder) and the direction (Directional EMG decoder) of the upcoming step.

Methods and materials: We validated a preliminary version of the approach by acquiring EMG signals from ten healthy subjects, performing steps in four directions (forward, backward, right, and left), in three different settings (ground-level walking, stairs, and ramps), and in both steady-state and static conditions. Both the Toe-off intention and Directional EMG decoders have been tested with a 5-fold cross-validation repeated five times, using linear and radial-basis-function kernels, and by changing the classification output timing, from 200 ms before to 50 ms after the toe-off.

Results: The Toe-off intention decoder reached a median accuracy of 83.34 % (interquartile range (IQR): 6.48) and specificity of 92.72 % (IQR: 3.62) in its radial-basis-function version, while the Directional EMG decoder's median accuracy ranged between 73.92 % (IQR: 5.8), 200 ms before the toe-off, to 92.91 % (IQR: 4.11), 50 ms after the toe-off, with the radial-basis-function kernel implementation. For both the Toe-off intention and Directional EMG decoders the radial-basis-function version achieved better performances than the linear one (Wilcoxon signed rank test, $p < 0.05$).

Conclusions and significance: The combination of the two decoders proved to be a promising solution to detect the step initiation and classify its direction, paving the way for wearable devices with a broader range of movements and more degrees of freedom, ultimately promoting usability in uncontrolled settings and better reactions to external perturbations. Additionally, the encumbrance of the setup is limited to the thigh of the leg of interest, which simplifies the implementation in compact devices, concurrently limiting the sensors worn by the subject.

1. Introduction

Lower limb pathologies can heavily impact the quality of life of a person, limiting his/her mobility and independence. Severe osteoarthritis, stroke-related lower limb impairments, neurodegenerative disorders, spinal cord injuries, and amputations are among the most common and invalidating conditions and the number of people suffering from them is expected to grow in the next decades [1,2], due to world population aging. Wearable devices, such as prostheses and exoskeletons, can help overcome mobility limitations caused by these health conditions, especially if able to provide net mechanical energy [3–5], mimicking the healthy leg behavior and limiting the adoption of harmful and energy-inefficient compensation strategies [6,7].

The above-mentioned robotic platforms are challenging in terms of both mechatronic and control system design; in particular, the control system must accomplish multiple tasks: recognizing the user's intent (high-level control), converting it into the desired device state (mid-level control) and actuating the device (low-level control) [8]. Implementing an efficient high-level control strategy promotes ownership, agency, embodiment, and usability, decreasing the risk of early

* Corresponding author.
E-mail address: eugenio.anselmino@santannapisa.it (E. Anselmino).

https://doi.org/10.1016/j.cmpb.2024.108305
Received 20 February 2024; Received in revised form 10 June 2024; Accepted 24 June 2024
Available online 24 June 2024

abandonment, which is a well-known issue for prostheses [9]. High-level control approaches adopting biomechanical (e.g., inertial measurement units) [8], surface electromyographic (sEMG) [10], and central [11] or peripheral [12,13] nervous system interfaces have been widely studied, showing promising results in the research environment. Such methods can discriminate different locomotion modalities or gait phases and can detect movement intention and onset by leveraging finite-state machine or machine learning (ML) techniques. sEMG is widely used for both locomotion mode classification [14] and movement onset detection [15–17] since it is possible to exploit preparatory movements and muscular activity, which can anticipate muscle contraction by up to 80 ms [16]. In addition, sEMG activity decoding allows the prediction of gait events such as toe-off (TO) up to 220 ms in advance [17], or the prediction of joint angles, such as the knee one, up to 100 ms in advance, as suggested in the preliminary results of [18]. Muscle activity can be leveraged by both finite-state control architectures [19] and ML-based algorithms, but despite the first approach being the most common due to the non-linearity and non-stationarity of sEMG signals, ML approaches represent the most promising solution due to their ability to detect the user's intent before the actual movement. Finite-state architectures fall short in detecting user's intentions because the decision criteria are generally manually selected by an operator, as in the case of commercial myoelectric hand prostheses. Consequently, finite-state architectures can not leverage small signal variations as optimally as ML approaches. Ankle-foot prostheses are a good representation of such dichotomy since sEMG signals can be used to switch states [20,21] or modulate torque parameters [22,23] in finite-state machine prosthetic ankles, but also to draw intended movements with ML [24].

Despite high-level control being essential for smooth human-machine interaction, state-of-the-art approaches are distant from replicating the complexity of human gait, especially in uncontrolled settings [25], such as uneven terrains or crowded places. In the literature, sEMG is widely used for predicting the onset of movement and its features (e.g., joint torques, joint angles) for both upper [15,16] and lower limbs [18,26] applications. For example, [17] demonstrated the possibility of detecting heel strike (HS) and TO events 130–260 ms in advance in transfemoral amputees using sEMG and kinematic data during forward ground-level walking. Nevertheless, while with kinematic signals was possible to predict the TO only when the prosthesis was leading (i.e., the prosthetic leg is moving first), with sEMG was possible to do it for both the leading and trailing (i.e., the healthy leg is moving first) cases. Despite their precision in predicting the user's intention, the known control algorithms only consider a frontal walking direction, both as regards locomotion mode classification and movement onset detection, limiting the usability of the devices in settings where abrupt direction changes are needed due to obstacles or external perturbations [27]. Turn detection algorithms partially assess the issue, detecting the intention of performing a turn during ground-level walking [28–30] or from a standing position [31]. They generally rely on kinematic data of the upper (e.g., head, trunk) [28–30,32] or lower (e.g., shank, ankle) [28,31] body, and are developed for assistive robotic or diagnosis applications. Although they are proven to enhance human-robot interactions [30], such algorithms only consider turning movements performed during ground-level walking, neglecting backward and lateral steps. In the literature, algorithms that consider lateral movements for exoskeleton control are present [33,34], but they mostly focus on step width adaptation to improve balance during ground-level walking tasks. [33] is the only work explicitly considering lateral steps, allowing the user to initiate the movement by controlling the Center of Mass (CoM) position. The CoM position is estimated through the upper body orientation, which represents a limitation for integration in devices worn exclusively on lower limbs (e.g., prostheses).

Ultimately, it is important to consider a more realistic scenario, in which the device user is free to move in multiple directions and perform different tasks (e.g., ground-level walking, stairs and ramps ascending and descending), concurrently limiting the setup encumbrance to the lower limbs. For these reasons, we developed and tested a novel sEMG-based intention detection algorithm (see "Directional EMG decoder" section), capable of predicting the upcoming step direction, and a TO intention decoder (see "Toe-off intention decoder" section), able to detect the movement onset independently from the step direction. Contrary to what is presented in the literature, our setup encumbrance is limited to a single leg and the approach has been tested on ground-level walking, stairs, and ramps scenarios. The combined use of these decoders is expected to improve the controllability of lower limb wearable devices, which will be able to support the user's movements adapting the assistance depending on the intended step direction [27].

1.1. Design of a directional EMG decoder

We categorized the possible leg movements into four classes (Fig. 1), based on four types of steps that can be performed in real-life scenarios: forward step (FW), backward step (BW), right step (R), and left step (L). Such categorization allows a good compromise in terms of the subject's mobility and algorithm complexity. For each class, it is necessary to explain some practical considerations that can impact the final implementation of the control framework:

- Forward (FW) step: performing a step forward is an action that can be performed in multiple settings (e.g., stairs, ramps, etc.) and, unlike the others, both during steady-state walking (i.e., subsequent steps are taken without stopping) and static tasks (i.e., performing one step from a standing position). This has two important implications: firstly, a realistic dataset is highly unbalanced toward the forward step class; secondly, during steady-state walking the only possible class is a forward step since it is very unlikely to abruptly change direction in such a case.
- Backward (BW) step: a backward step can be performed in multiple settings (e.g., stairs, ramps, etc.), but only statically; the rationale behind this choice is that, for a subject, it is very unlikely in a realistic scenario to take multiple backward steps subsequently.
- Right (R) and left (L) steps: lateral steps can be performed, as backward ones, only statically, with the difference that the only possible locomotion modality is ground-level walking. This claim can be easily justified by the fact that is highly improbable for a user to climb a stair or approach a ramp with a lateral step.

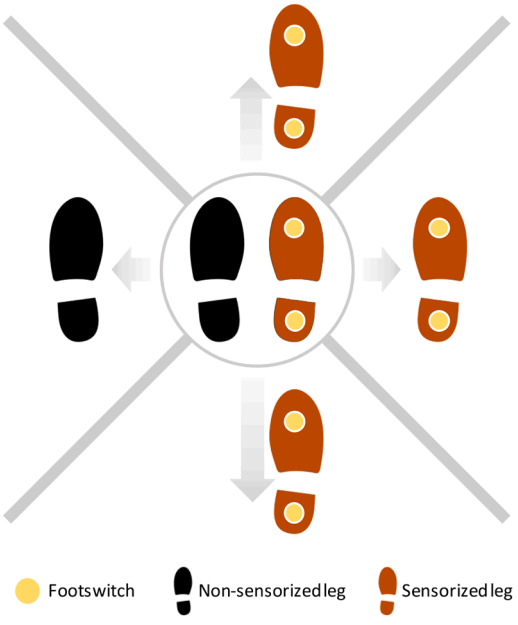

Fig. 1. Possible steps to be taken into account for the directional EMG decoder.

Such discretized movements have been considered only for the right side both because we wanted to consider the case of unilateral devices (e.g., prostheses, orthoses), and because the approach can be easily mirrored to the left side if needed. As shown in Fig. 1, the first leg to be moved is always the sensorized one (i.e., the right one) except for the left step, in which the left leg is moved first. This choice was made to avoid crossing steps, which are uncommon in normal daily living situations.

As shown in Fig. 2, the leg direction classifier is supposed to provide the classification output after the detection of a movement intention, during the late-stance phase of the gait, and no further than the TO, to allow the device to correctly assist the subject during the push-off depending on the desired movement direction. Due to the interaction between the directional EMG and the movement intention classifiers, in this work we also propose a TO intention decoder that has been trained and tested on steps taken in all the four directions discussed above. Furthermore, this classification time frame can enhance the performance of the adopted locomotion mode classifier, allowing the prediction to be performed only on the subset of classes suitable for the detected direction of the step. For locomotion mode classifier we intend the algorithm responsible for classifying the task the subject wants to perform, intended as walking modality (e.g., typical locomotion modes can be: ground-level walking, ramps ascending, stairs descending, etc.). However, this interaction between leg direction and locomotion mode classifiers is only possible during the gait's late-stance phase, as the directional EMG decoder is invoked close to the TO instant only. Nevertheless, for some applications (e.g., lower limb prostheses) the locomotion mode needs to be identified close to the HS instant to provide assistance during the stance phase of the gait. Therefore, it is not possible to leverage the directional EMG decoder output to further improve the locomotion mode classification.

2. Materials and methods

Ten healthy subjects have been enrolled to participate in the study, five men and five women, aged between 23 and 35. The experimental protocol has been approved by the Joint Ethical Committee of Scuola Superiore Sant'Anna and Scuola Normale Superiore (protocol number: 18/2023). Subjects were informed about the experimental procedures before the start of the session and signed a written consent form approved by the ethical committee.

2.1. Experimental setup and protocol

Experimental sessions occurred at the Biorobotics Institute of Scuola Superiore Sant'Anna (Pisa, Italy), with the subject moving in commonly used environments. After the introduction of the experimental protocol, participants were asked to wear the instrumentation on the right leg as shown in Fig. 3 (left): four pre-gelled sEMG electrodes were placed on the Biceps Femoris, Tensor Fasciae Latae, Rectus Femoris, and Adductor, together with two footswitches placed under the sole of the shoe, respectively under the heel and the toe. Target muscles were chosen accordingly to [10], in which they proved to provide gait-related reliable information for ML applications concurrently limiting the setup burden. The choice was also guided by the need to have muscular activations representative of the abduction and adduction movements of the leg, which are essential during the R and L steps described above. The Adductor is indeed responsible for the adduction movement of the thigh, while the Tensor Fasciae Latae is an abductor of the hip joint [35]. The EMG recordings were carried out with a bipolar setting, using two pre-gelled electrodes for each muscle with an 8 mm active site and 25 mm inter-electrode distance. The purpose of the footswitches was to allow the identification of the relevant gait events (i.e., TO and HS), necessary for successive analyses. The signals were recorded using the Sessantaquattro portable system by OT Bioelettronica (Torino, Italy), at a sample frequency of 2 kHz.

Each subject was asked to perform a total of seven sessions containing FW, BW, R, and L steps, both in static and steady-state conditions when possible (see "Key concepts for a Directional EMG decoder" section); a detailed description of each session is presented below:

- Session 1: the subject performs alternated FW and BW steps statically in a ground-level setting; a total of 60 steps was acquired.
- Session 2: the subject performs alternated R and L steps statically; a total of 120 steps was acquired.
- Session 3: the subject performs alternated FW and BW steps on stairs statically; a total of 60 steps was acquired.
- Session 4: the subject performs alternated FW and BW steps on ramps statically; a total of 60 steps was acquired.
- Session 5: the subject performed steady-state FW steps in a ground-level setting; a total of 30 steps was acquired.
- Session 6: the subject performed steady-state FW steps ascending and descending flights of stairs, the subject was asked to stop after each flight of stairs only, alternating the ascending and descending condition; a total of 60 steps was acquired, 30 for each condition.
- Session 7: the subject performed steady-state FW steps ascending and descending ramps, the subject was asked to stop after each ramp only, alternating the ascending and descending condition; a total of 60 steps was acquired, 30 for each condition.

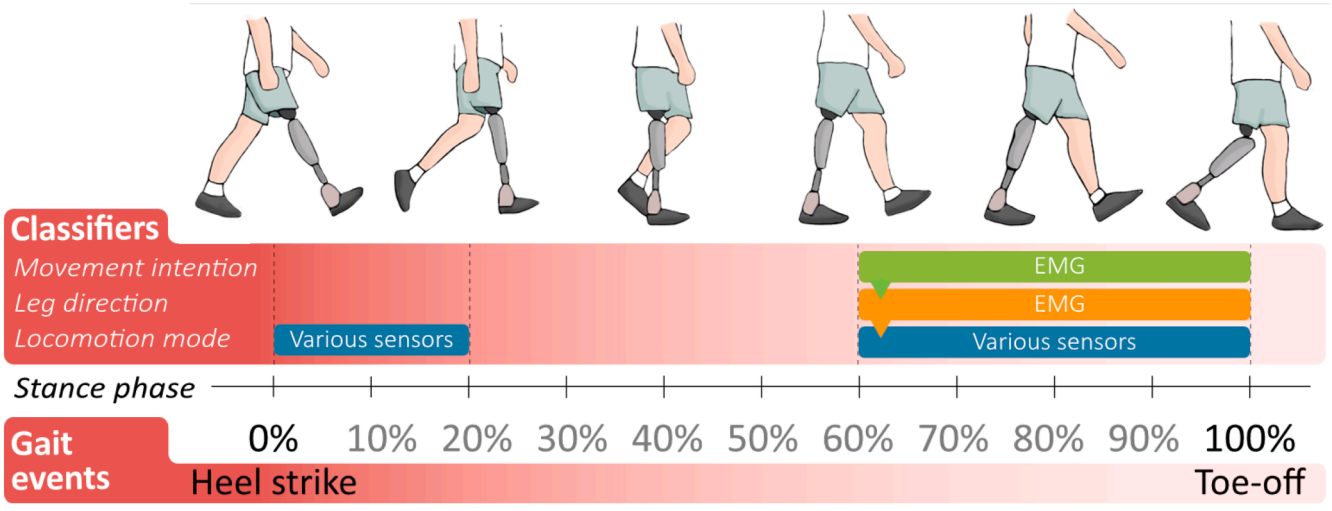

Fig. 2. Example of timing of the classification output of the classifiers generally involved in the control of a lower limb device; in this work only the movement intention and leg direction classifiers are studied. For the sake of the example the instrumented leg is depicted as a prosthesis.

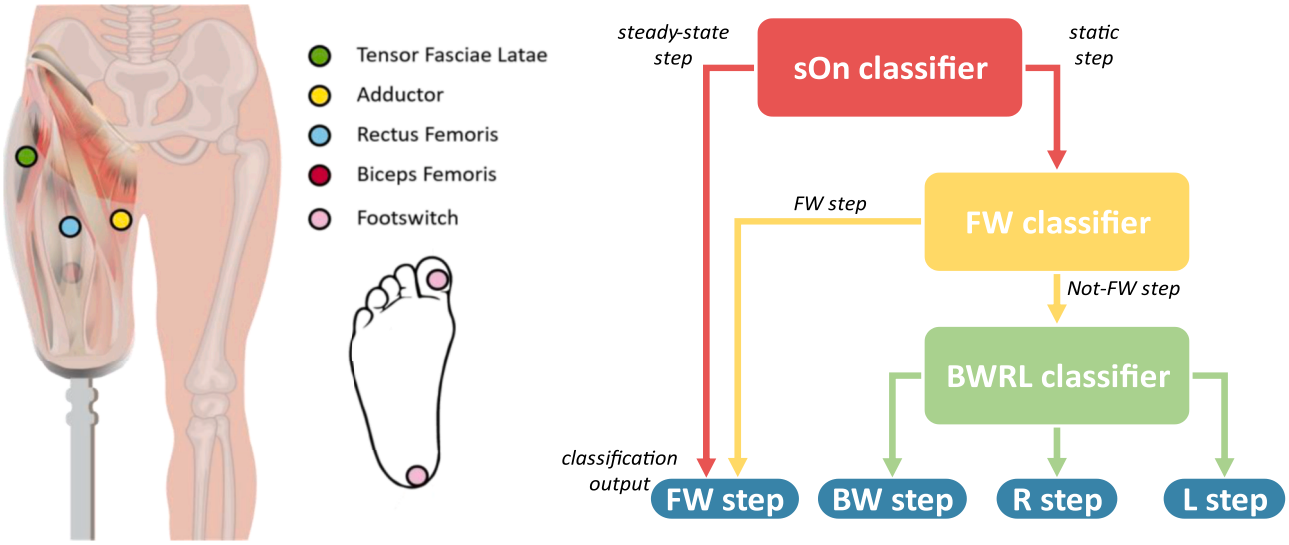

Fig. 3. Position of the sEMG electrodes, for the sake of the example the instrumented leg is depicted as a prosthesis (left); scheme of the directional EMG decoder and its subcomponents (right).

The sessions had an average duration of five minutes each and occurred subsequently in a single day, interspersed by 5 min of rest. The number of steps for each session was selected to balance the final class numerosity (i.e., FW, BW, R, L steps), the number of steps for each condition (e.g., static steps on stairs, steady-state steps on ramps, etc.), and experimental session duration. Nevertheless, as explained in the "Directional EMG decoder" section, it is important to consider that in a realistic setting there is a predominance of steady-state and FW steps, which the decoder must take into account, and consequently the composition of the acquired dataset reflects this imbalance. The rationale behind the acquisition of steps during stairs, ramps, and ground-level walking is to allow the decoders to be naïve about the setting in which the step is taken.

2.2. Data processing

Acquired sEMG signals were filtered using a bandstop filter between 48 Hz and 52 Hz, and a bandpass filter between 20 Hz and 500 Hz. The Mean Absolute Value (MAV) was selected as a feature, extracting it through a 20 ms moving window with a 15 ms overlap. TO and HS events were extracted from footswitch signals and visually inspected to remove eventual outliers. Gait events inspection and selection operation was carried out on a custom MATLAB graphical user interface (MATLAB R2022b, MathWorks). Signal filtering, feature extraction, and decoder training, testing, and validation were performed offline on a workstation (i7–12,700, 16 GB RAM) using custom Python scripts (Python v3.7.16).

2.3. Toe-off intention decoder

The TO intention decoder is based on a single error-correcting-output-codes (ECOC) support-vector-machine (SVM) (scikit-learn v0.23.1), chosen due to its generalization ability with small datasets and its potential real-time portability. The classifier objective is to determine if a TO will be performed in the next 200 ms. The input is the standardized MAV computed from the four sEMG signals in a window of 200 ms preceding the classifier call, and the output is provided every 50 ms in the time frame between the HS and the TO. The length of the window has been selected according to [17], in which muscular activity is detected up to 200 ms before the TO. To minimize false positives, the output sequence is post-processed and a TO intention is detected only if 3 of the last 4 classifications recognized the intention of initiating a step.

The decoder is subject-specific, and has been tested by performing a subject-wise 5-fold cross-validation repeated 5 times, using footswitches signals as ground truth for TO instants identification. The test was repeated for two SVM kernels, linear and radial-basis-function (RBF), and at each iteration a grid search was performed to select the best regularization parameter, chosen between a subset of values (0.001, 0.01, 0.1, 1, 10, 100, 1000). The analysis has been performed offline. Wilcoxon signed rank test (WSRT) was performed to compare different conditions. Results are presented in the median (IQR: interquartile range) format.

2.4. Directional EMG decoder

The directional EMG decoder is a hierarchic classifier based on three ECOC SVM sub-classifiers: the "*steady or not-steady*" classifier (sOn), which discriminates between a steady-state gait and static steps; the "*forward or not-forward*" classifier (FW), which discerns between FW steps and BW, R, L steps; and the "*backward or right or left*" classifier (BWRL), which discriminated between BW, R and L steps. The rationale behind this division is that in a realistic dataset, there is a predominance toward steady-state and FW steps, and therefore is of primary importance to correctly classify these conditions leveraging all the available data for the training phase of the algorithm.

The *sOn classifier* takes as input the standardized MAV extracted from signals of the second before the classification instant, classifying if the upcoming step will be a static or steady-state one. This is the first classifier invoked after a movement intention is detected: if its output states that the upcoming step will be a steady-state one, only an FW step will be possible and no other classifier will be invoked.

The *FW classifier* is the second in order of invocation and takes as input the standardized MAV of the 200 ms before the classification instant. The length of the input window has been chosen based on the results presented in [17], which detects muscular activity up to 200 ms before the TO event. The FW classifier has two possible outputs: FW step, in which case the BWRL classifier is not invoked; or not-FW step, in which case the BWRL classifier is called.

The *BWRL classifier* is the last to be invoked and as the FW one takes as input the standardized MAV of the 200 ms before the classification instant. The classification output corresponds to a BW, R, or L step.

The three classifiers are subject-specific and have been tested singularly and together, in the final form of the hierarchic classifier (Fig. 3, right), by performing a subject-wise 5-fold cross-validation repeated 5 times and varying the classification output time from 200

ms before the TO to 50 ms after, with steps of 5 ms. The test was repeated for two SVM kernels, linear and RBF, and at each iteration a grid search was performed to select the best regularization parameter, chosen between a subset of values (0.001, 0.01, 0.1, 1, 10, 100, 1000). The output of the hierarchic classifier has been computed by selecting the best-performing single classifier given the output instant and the kernel. The analysis has been performed offline. Wilcoxon signed rank test (WSRT) was performed to compare different conditions. Results are presented in the median (IQR: interquartile range) format.

2.5. Real-time portability

To validate the online portability of the proposed decoders, we measured the inference time of each classifier involved in the classification pipeline, for one subject and one classification instant (50 ms before TO). The test was performed on a Google Coral Developer Board (NXP i.MX 8 M SoC CPU, 1GB RAM, Python v3.7.3) and repeated until each classifier performed 10,000 classifications for each kernel type.

3. Results

As shown in Fig. 4, the accuracy of the TO intention decoder is 72.69 % (IQR: 3.54) for the linear kernel version and 83.34 % (IQR: 6.48) for the RBF one. Both kernels reach a recognition rate above 90 % for the absence of intention (i.e., true negatives), but the RBF one shows a higher precision regarding the recognition of TO intention with 72.48 % (IQR: 11.47). The results imply greater usability of the RBF kernel version of the algorithm, which shows better overall performances (WSRT, $p < 0.05$) maintaining a lower level of false positives (WSRT, $p < 0.05$), essential to avoid potentially detrimental step initiations.

The accuracies of the sOn, FW, and BWRL classifiers are presented in Fig. 5 (left), with the accuracy expressed with the f1-score metric and the variability with IQR. The sOn classifiers show stable accuracies of around 95 % along the whole window of interest, with no statistically significant differences between the two kernel implementations (WSRT, $p > 0.05$). A degradation of performance is present for both the FW and BWRL classifiers with earlier classification outputs, with a median accuracy of around 80 % 200 ms before the TO to above 90 % 50 ms after the TO. In the FW case, the RBF kernel of the algorithm overperforms the linear one (WSRT, $p < 0.05$); while in the BWRL case, no statistically significant differences are observed between the two kernels (WSRT, $p > 0.05$).

The accuracies of the hierarchic classifier are shown in Fig. 5 (right) and Fig. 6. As for the FW and BWRL classifiers, a similar degradation of the performances is noticeable with the anticipation of the classification output, with median accuracies ranging from 70 % 200 ms before the TO to more than 90 % 50 ms after the TO. The RBF kernel version of the classifier outperforms the linear one (WSRT, $p < 0.05$), with an accuracy ranging between 73.92 % (IQR: 5.8), 200 ms before the toe-off, to above 92.91 % (IQR: 4.11), 50 ms after the toe-off. As presented in Fig. 6, the RBF hierarchic algorithm detects an FW step with an accuracy above 90 %, while for BW, R, and L steps the performances are lower, with accuracies between 75 % to 90 % depending on the classification instant. As shown in Fig. 7, given the kernel and classification instant, the hierarchic classifier does not show statistically significant differences (WSRT, $p > 0.05$) in classification accuracy across the different locomotion tasks (i.e., ground-level walking, stairs ascending and descending, ramps ascending and descending). The median accuracies for the population range from 68.84 % to 93.13 % depending on the locomotion task and the classification instant.

As shown in Fig. 8, the linear kernel version of each classifier is significantly faster than the RBF counterpart (WSRT, $p < 0.05$) in providing the classification output. The FW and BWRL classifiers have an inference time that never exceeds 0.75 ms, with a median classification time of 0.6 ms and 0.59 ms respectively. The sOn classifier and the classifier used for the TO intention decoder have an inference time that never exceeds 3.55 ms, with a median classification time of 3.37 ms and 2.74 ms respectively.

4. Discussion

We developed, tested, and validated two novel decoders meant to be implemented into existing high-level controls of wearable lower-limb devices, with the objective of better mimicking the ability of humans to perform steps in multiple directions. Despite not being widely studied in the literature, “non-frontal” steps are crucial for locomotion in crowded places and uneven terrain, and for reacting to external perturbations [27]; moreover, allowing a wider range of controllable movements could promote embodiment and usability of wearable devices in uncontrolled settings. We presented a TO intention decoder independent of the direction of the step, unlike previous works present in literature, and a novel EMG decoder able to classify the direction of the upcoming step. The two classification algorithms have been tested by acquiring data from ten healthy subjects, sensorized with four sEMG electrodes and performing both static and steady-state tasks on stairs, ramps, and ground-level walking. Their predictive accuracy was studied by varying classification output instant and SVM kernel typology.

As presented in the “Results” section, the *TO intention decoder* shows an overall classification accuracy of 83.34 % in the RBF kernel version, but a far more interesting 92.72 % specificity, making it preferable to the

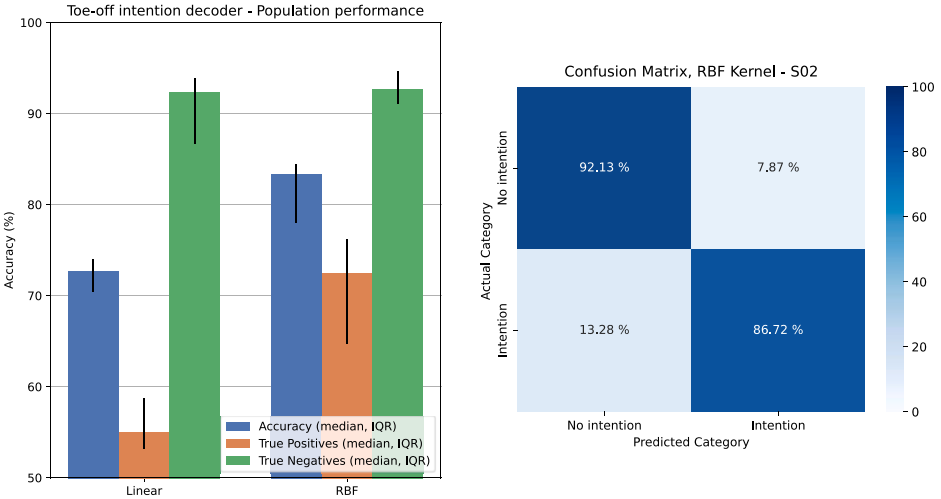

Fig. 4. Average performance of the TO intention decoder on the population, for linear and RBF kernel (left); example of confusion matrix for a single subject (right).

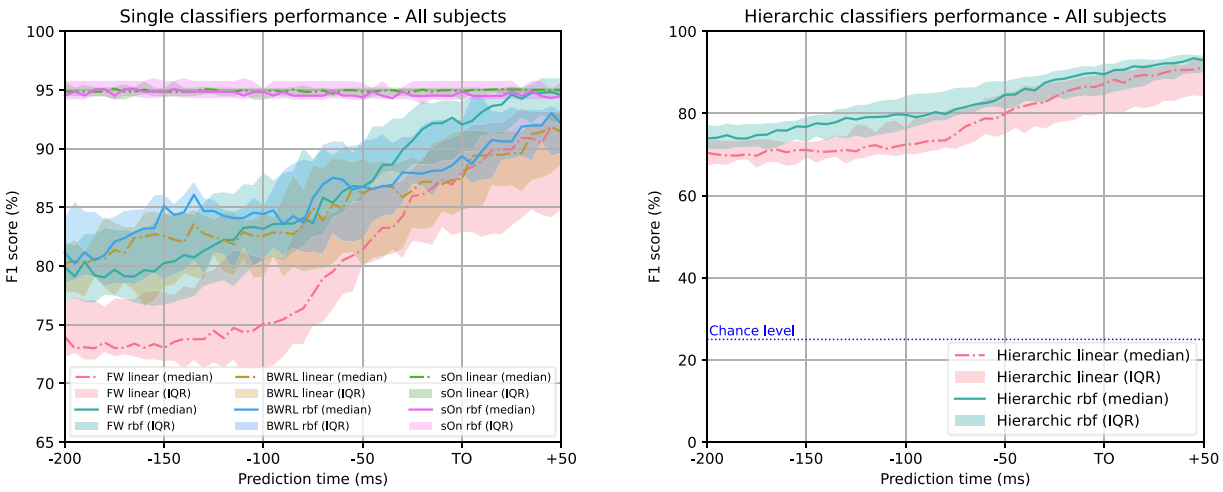

Fig. 5. Performance of the single classifiers composing the directional EMG decoder (left); performance of the hierarchic classifier (right).

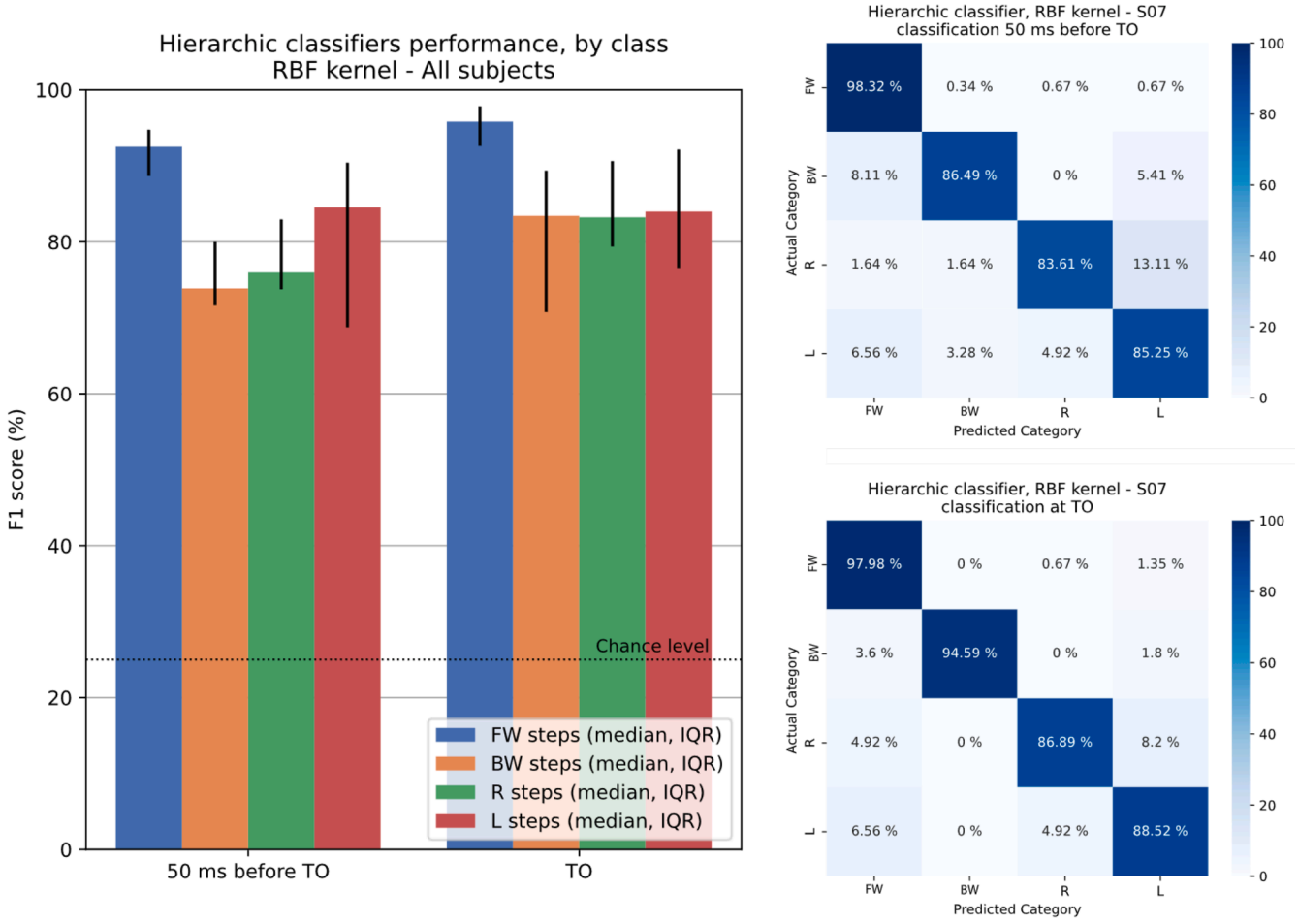

Fig. 6. Classification performance of the hierarchic classifier for each step direction, at TO and 50 ms prior the TO (left); example confusion matrixes of the hierachic classifier for a single subject, at TO and 50 ms prior the TO (right).

linear kernel implementation. Having a low false positive rate is crucial for this application since from the point of view of usability and safety is preferable to avoid false step initiations of the wearable device, which could unbalance the user causing potentially harmful falls. Furthermore, spurious device activations could increase the risk of early abandonment, which is a known issue for specific populations (e.g., prostheses users). The *directional EMG decoder* shows accuracies above 75 % across the output window of interest, reaching an accuracy above 90 % close to the TO and with the RBF kernel version, which outperforms the linear kernel implementation, especially for early output instants. The algorithm presents noticeably higher performances in classifying FW steps if compared to the other classes; this implies a high capability in detecting the type of steps that show a higher degree of risk, being performed dynamically, and that are more likely to happen in a real-life scenario.

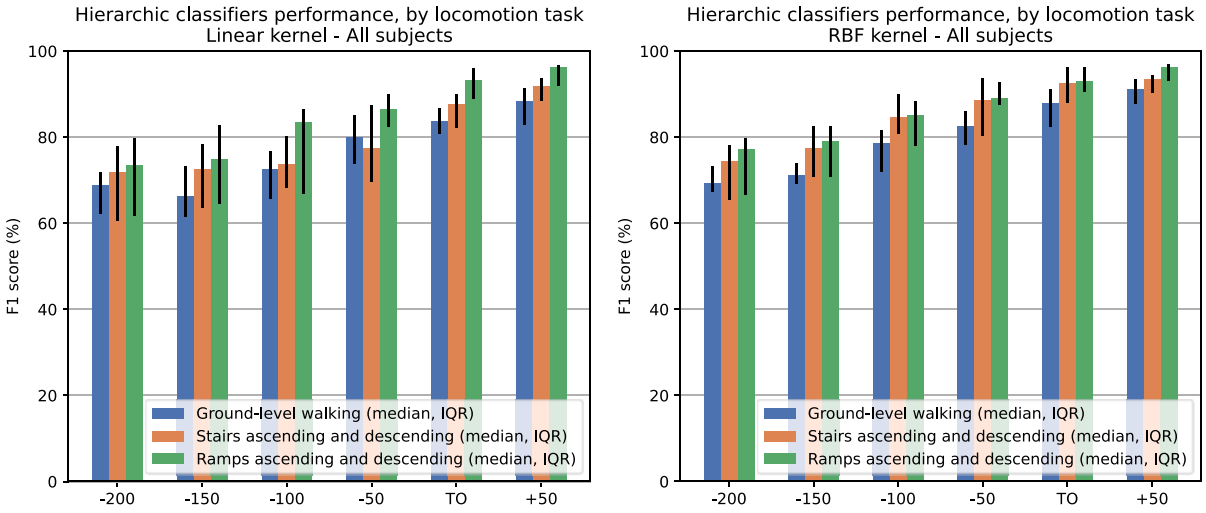

Fig. 7. Classification performance of the hierarchic classifier for each locomotion task (ground-level walking, stairs ascending and descending, ramps ascending and descending). The chart shows the classification performances for all the directional steps possible during the locomotion task considered.

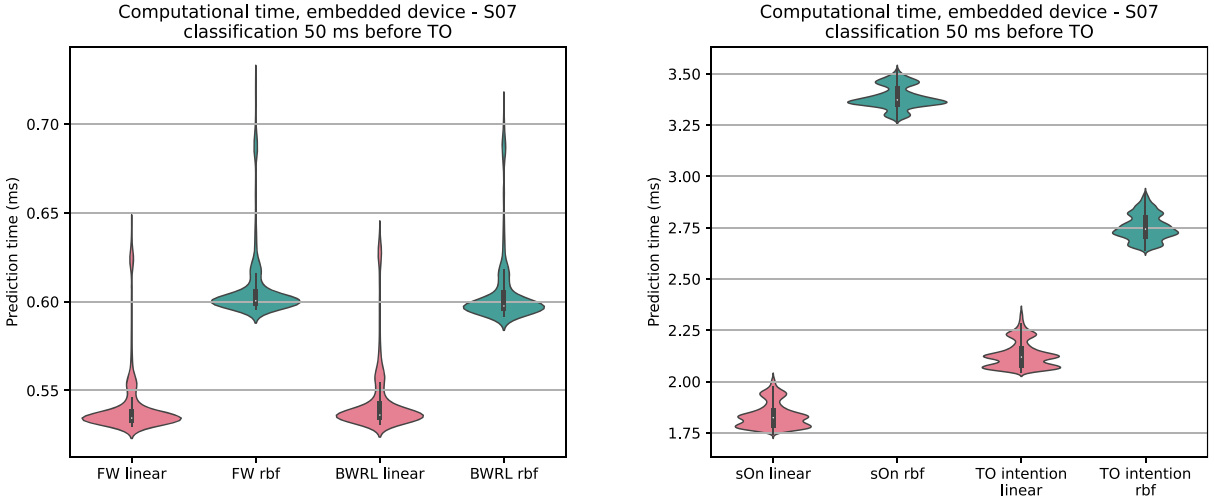

Fig. 8. Computational time required for the inference of the classifiers proposed; for the sake of the example, we run the test on one subject, assuming the classification to happen 50 ms before the TO. Results for both the linear and rbf versions of the classifiers are presented.

The reasons behind the discrepancy in classification accuracy of the different types of steps are multiple: first, the dataset mimics the composition of a realistic dataset and therefore FW steps are the most represented to the detriment of BW, R, and L steps (see "Experimental setup and protocol" section); secondly, the muscles responsible for the abduction and adduction of the hip joint play also a role in the stabilization of the leg during forward walking [35]. This stabilization role can cause muscular activations during forward walking tasks, increasing the chance of misclassifications. The algorithm does not present different performances across different locomotion tasks (i.e., ground-level walking, stairs ascending and descending, ramps ascending and descending), confirming its robustness with respect to the setting in which the step is performed.

The classifiers involved in the directional EMG and TO intention decoders showed inference times shorter than 3.55 ms, confirming the portability of such an approach on embedded computing platforms. Despite the linear versions of the algorithms being faster than their RBF counterparts, the adoption of the latter is generally justified by the noticeable increase in classification accuracy at the expense of an increase in inference time of a maximum of 1.5 ms. The only exceptions are the sOn and BWRL classifiers, of which both kernel versions have comparable classification performances. Ultimately, the combination of the two decoders represents a promising approach to developing more usable lower-limb wearable devices, taking into account a broader range of movements and increasing the degrees of freedom available to the user.

Our decoders can have several applications. Modern *lower limb prostheses* could benefit both in terms of usability and embodiment of the algorithms proposed, which can provide smoother control over the prosthetic leg together with additional mobility. The possibility of flawlessly performing lateral and backward steps can also help in engaging activities in more challenging environments, providing more stability to the user and the ability to better react to external perturbations (e.g., a bump with a person). Ultimately, a more stable and controllable prosthesis would promote an active lifestyle, reducing the risk of insurgence of comorbidities. Nevertheless, it is important to point out that the majority of commercial prostheses present passive ankle mechanisms, which allow only plantar flexion and dorsiflexion; it would be therefore necessary to modify the directional EMG decoder to discriminate only between forward and backward steps (i.e., without implementing the BWRL classifier). It is also worth mentioning that the classification output of the directional EMG decoder must anticipate the TO to allow the assistance of the push-off movement. For similar reasons, o*rthoses and exoskeletons* could benefit from the implementation of

the proposed decoders in their high-level controls, increasing the range of motion and usability, and obtaining better stability on uneven terrains and in reactions to perturbations. However, both decoders could necessitate modifications depending on the subject's joints assisted by the device; such as in the case of hip orthoses and exoskeletons, for which would be possible to provide the directional EMG decoder output near or after the TO instant since the push-off is managed by subject, contrary to what happens for prostheses user. It is important to point out that different applications bring different requirements in terms of safety, depending on the level of assistance provided to the subject. As an example, a hip exoskeleton, intended to be used with mildly impaired subjects to improve their metabolic economy, presents a lower degree of risk if compared to a transfemoral prosthesis. A classification error, if performed with a hip exoskeleton on a subject able to stand and walk autonomously, would lead to discomfort rather than a fall, contrary to the case of lower limb prostheses.

In conclusion, the combined use of the two presented decoders would allow the development of more effective high-level controllers, capable of guaranteeing a broader range of movements and ultimately enhancing the use of a broad range of wearable devices in realistic settings. The setup adopted is compact and limited to one leg, which allows the implementation in compact devices, concurrently limiting the sensors worn by the subject. Further developments are possible, both in terms of classification accuracy and approach validation. Regarding the first, sensor fusion techniques involving inertial motion units (IMUs) and high-density sEMG will be tested, to increase the amount of information available for the algorithm training. In particular, IMUs proved to be a source of valuable information for locomotion mode classification [10], gait assessment applications [35], and gait event prediction [17]. Sensor fusion approaches can also help in mitigating the time-varying and non-stationary nature of sEMG signals, that are responsible for the subject specificity of the current iteration of the presented algorithm. Leveraging additional data sources can help close the gap towards a subject-independent directional EMG decoder. In addition, the classifiers will be tested for specific applications (e.g., prostheses users, exoskeletons), in less controlled settings (e.g., crowded places), and with multiday acquisitions on the same subject to study the long-term robustness of the proposed approach. Further developing application and patient-specific versions of the presented control framework will be essential to fully validate these algorithms in realistic settings. Nevertheless, it is important to point out that such specific implementations will largely depend on the target population and hardware adopted by future studies; for example, the classification algorithm may vary greatly depending on the degrees of freedom allowed by an exoskeleton.

Availability of data and materials

The data that support this study are not openly available due to ethical and privacy concerns.

Funding

This work was supported in part by the Bertarelli Foundation, by INAIL (Centro Protesi, Vigorso di Budrio, Italy) under project PR19-PAI-P2 MOTU++, by National Recovery and Resilience Plan - Italian Ministry of University and Research - European Union – NextGenerationEU under projects MNESYS and THE.

Ethics approval and consent to participate

The experimental protocol has been approved by the Joint Ethical Committee of Scuola Superiore Sant'Anna and Scuola Normale Superiore (protocol number: 18/2023). Subjects were informed about the experimental procedures before the start of the session and signed a written consent form approved by the ethical committee.

CRediT authorship contribution statement

Eugenio Anselmino: Writing – review & editing, Writing – original draft, Visualization, Validation, Methodology, Formal analysis, Data curation, Conceptualization. **Alberto Mazzoni:** Writing – review & editing, Supervision, Resources, Project administration, Funding acquisition, Formal analysis. **Silvestro Micera:** Writing – review & editing, Supervision, Resources, Project administration, Formal analysis.

Declaration of competing interest

The authors declare that they have no known competing financial interests or personal relationships that could have appeared to influence the work reported in this paper.

Acknowledgment

None.

References

[1] B. Ovbiagele, L.B. Goldstein, R.T. Higashida, V.J. Howard, S.C. Johnston, O. A. Khavjou, et al., Forecasting the future of stroke in the united states: a policy statement from the American heart association and American stroke association, Stroke 44 (8) (2013) 2361–2375.
[2] K. Ziegler-Graham, E.J. MacKenzie, P.L. Ephraim, T.G. Travison, R. Brookmeyer, Estimating the prevalence of limb loss in the United States: 2005 to 2050, Arch. Phys. Med. Rehabil. 89 (3) (2008) 422–429.
[3] D.H. Gates, J.M. Aldridge, J.M. Wilken, Kinematic comparison of walking on uneven ground using powered and unpowered prostheses, Clin. Biomechan. 28 (4) (2013) 467–472.
[4] H.M. Herr, A.M. Grabowski, Bionic ankle-foot prosthesis normalizes walking gait for persons with leg amputation, Proceed. Roy. Soc. B: Biolog. Sci. 279 (1728) (2012) 457–464.
[5] A. Esquenazi, M. Talaty, A. Packel, M. Saulino, The Rewalk powered exoskeleton to restore ambulatory function to individuals with thoracic-level motor-complete spinal cord injury, Am. J. Phys. Med. Rehabil. 91 (11) (2012) 911–921.
[6] D.S. Pieringer, M. Grimmer, M.F. Russold, R. Riener, Review of the actuators of active knee prostheses and their target design outputs for activities of daily living, in: IEEE International Conference on Rehabilitation Robotics, IEEE Computer Society, 2017, pp. 1246–1253.
[7] J. Mendez, S. Hood, A. Gunnel, T. Lenzi, Powered knee and ankle prosthesis with indirect volitional swing control enables level-ground walking and crossing over obstacles, Sci. Robot 5 (2020). Available from, https://www.science.org.
[8] M.R. Tucker, J. Olivier, A. Pagel, H. Bleuler, M. Bouri, O. Lambercy, et al., Control strategies for active lower extremity prosthetics and orthotics: a review, J. Neuroeng. Rehabil. 12 (2015). Available from: http://www.jneuroengrehab.com/content/12/1/1.
[9] L. Paternò, M. Ibrahimi, E. Gruppioni, A. Menciassi, L. Ricotti, Sockets for limb prostheses: a review of existing technologies and open challenges, IEEE Trans. Biomed. Eng. 65 (9) (2018) 1996–2010.
[10] F. Barberi, F. Iberite, E. Anselmino, P. Randi, R. Sacchetti, E. Gruppioni, et al., Early decoding of walking tasks with minimal set of EMG channels, J. Neur. Eng. (2023), https://doi.org/10.1088/1741-2552/acc901. Available from:.
[11] D. Novak, R. Riener, A survey of sensor fusion methods in wearable robotics. Robotics and Autonomous Systems, Elsevier B.V., 2015, pp. 155–170.
[12] Atakan Varol H., Goldfarb M. Decomposition-Based Control for a Powered Knee and Ankle Transfemoral Prosthesis, IEEE 10th International Conference on Rehabilitation Robotics (2007):783-789.
[13] D. Farina, I. Vujaklija, R. Brånemark, A.M.J. Bull, H. Dietl, B. Graimann, et al., Toward higher-performance bionic limbs for wider clinical use, Nat. Biomed. Eng. 7 (2023) 473–485.
[14] Fleming A., Stafford N., Huang S., Hu X., Ferris D.P., Huang H.H. Myoelectric control of robotic lower limb prostheses: a review of electromyography interfaces, control paradigms, challenges and future directions. Vol. 18, J. Neural. Eng.. IOP Publishing Ltd; 2021.
[15] I.M. Khairuddin, S.N. Sidek, A.P.P.A. Majeed, M.A.M. Razman, A.A. Puzi, H. M. Yusof, The classification of movement intention through machine learning models: the identification of significant time-domain EMG features, PeerJ Comput. Sci. 7 (2021) 1–15.
[16] T. Lenzi, S.M.M. De Rossi, N. Vitiello, M.C. Carrozza, Intention-based EMG control for powered exoskeletons, IEEE Trans. Biomed. Eng. 59 (8) (2012) 2180–2190.
[17] E.C. Wentink, S.I. Beijen, H.J. Hermens, J.S. Rietman, P.H. Veltink, Intention detection of gait initiation using EMG and kinematic data, Gait Posture 37 (2) (2013) 223–228.
[18] Z. Ding, C. Yang, Z. Wang, X. Yin, F. Jiang, Online adaptive prediction of human motion intention based on semg, Sensors 21 (8) (2021).
[19] Dawley James, Fite Kevin. EMG Control of a Bionic Knee Prosthesis: exploiting Muscle Co-Contractions for Improved Locomotor Function, 2013 IEEE 13th

International Conference on Rehabilitation Robotics (ICORR), Seattle, WA, USA, (2013) pp. 1-6.
[20] S. Au, M. Berniker, H. Herr, Powered ankle-foot prosthesis to assist level-ground and stair-descent gaits, Neur. Netw. 21 (4) (2008) 654–666.
[21] B. Chen, Q. Wang, L. Wang, Adaptive slope walking with a robotic transtibial prosthesis based on volitional EMG control, IEEE/ASME Transact. Mechatron. 20 (5) (2015) 2146–2157.
[22] Wang J., Kannape O., Herr H. Proportional EMG control of ankle plantar flexion in a powered transtibial prosthesis, 2013 IEEE 13th International Conference on Rehabilitation Robotics (ICORR), Seattle, WA, USA, 2013, pp. 1-5.
[23] S. Huang, J.P. Wensman, D.P. Ferris, An experimental powered lower limb prosthesis using proportional myoelectric control, J. Med. Dev., Transact. ASME 8 (2) (2014).
[24] S.K. Au, P. Bonato, H. Herr, An EMG-position controlled system for an active ankle-foot prosthesis: an initial experimental study, in: Proceedings of the 2005 IEEE 9th International Conference on Rehabilitation Robotics, 2005, pp. 375–379.
[25] F. Barberi, E. Anselmino, A. Mazzoni, M. Goldfarb, S. Micera, Toward the development of user-centered neurointegrated lower limb prostheses, IEEE Rev. Biomed. Eng., vol. 17, pp. 212-228, (2023).
[26] E.C. Wentink, V.G.H. Schut, E.C. Prinsen, J.S. Rietman, P.H. Veltink, Detection of the onset of gait initiation using kinematic sensors and EMG in transfemoral amputees, Gait Post. 39 (1) (2014) 391–396.
[27] B.E. Maki, W.E. Mcilroy, S.D. Perry, Influence of lateral destabilization on compensatory stepping responses, J. Biomechan. 29 (1996).
[28] R.Z.U. Rehman, P. Klocke, S. Hryniv, B. Galna, L. Rochester, Din S Del, et al., Turning detection during gait: algorithm validation and influence of sensor location and turning characteristics in the classification of parkinson's disease, Sens. (Switzerl.) 20 (18) (2020) 1–24.
[29] D. Novak, M. Goršič, J. Podobnik, M. Munih, Toward real-time automated detection of turns during gait using wearable inertial measurement units, Sens. (Switzerl.) 14 (10) (2014) 18800–18822.
[30] I. Farkhatdinov, N. Roehri, E. Burdet, Anticipatory detection of turning in humans for intuitive control of robotic mobility assistance, Bioinspir. Biomim. 12 (5) (2017).
[31] C. Pew, G.K. Klute, Turn intent detection for control of a lower limb prosthesis, IEEE Trans. Biomed. Eng. 65 (4) (2018) 789–796.
[32] A.M. López, J.C. Alvarez, D álvarez, Walking turn prediction from upper body kinematics: a systematic review with implications for human-robot interaction, Appl. Sci. (Switzerl.). MDPI AG 9 (2019).
[33] L. Wang, S. Wang, E.H.F. van Asseldonk, H. van der Kooij, Actively controlled lateral gait assistance in a lower limb exoskeleton, in: 2013 IEEE/RSJ International Conference on Intelligent Robots and Systems, 2013, pp. 965–970.
[34] A. Alili, A. Fleming, V. Nalam, M. Liu, J. Dean, H. Huang, Abduction/adduction assistance from powered hip exoskeleton enables modulation of user step width during walking, IEEE Trans. Biomed. Eng. 71 (1) (2024) 334–342.
[35] N. Palastanga, R. Soames, Anatomy and Human Movement: Structure and Function, 6th ed., Churchill Livingstone, Edinburgh, 2012. Available from: http://lib.ugent.be/catalog/rug01:001703316.